

Article

Evaluation of Keratin/Bacterial Cellulose Based Scaffolds as Potential Burned Wound Dressing

Cezar Doru Radu ¹, Liliana Verestiuc ^{2,*} , Eugen Ulea ³, Florin Daniel Lipsa ³, Vasile Vulpe ⁴ , Corneliu Munteanu ⁵ , Laura Bulgariu ⁶ , Sorin Pașca ⁴ , Camelia Tamas ^{7,*}, Bogdan Mihnea Ciuntu ^{8,*}, Madalina Ciocan ⁴, Ionela Sîrbu ⁴, Elena Gavrilas ⁴, Ciprian Vasile Macarel ¹ and Bogdan Istrate ⁵

- ¹ Department of Chemical Engineering, Faculty of Industrial Design and Affairs Management, “Gheorghe Asachi” Technical University Iasi, Mangeron Street, No/29, 700050 Iasi, Romania; cezar-doru.radu@academic.tuiasi.ro (C.D.R.); macarelciprian@gmail.com (C.V.M.)
- ² Department of Biomedical Sciences, Faculty of Medical Bioengineering, “Grigore T. Popa” University of Medicine and Pharmacy, 11-16, M. Kogalniceanu Street, No. 9-13, 700454 Iasi, Romania
- ³ Faculty of Agriculture, “Ion Ionescu de la Brad” University of Agricultural Sciences and Veterinary Medicine, M. Sadoveanu Alley, No. 3, 700490 Iasi, Romania; eulea@uaiasi.ro (E.U.); flipsa@uaiasi.ro (F.D.L.)
- ⁴ Faculty of Veterinary Medicine, “Ion Ionescu de la Brad” University of Agricultural Sciences and Veterinary Medicine, M. Sadoveanu Alley, No. 8, 700489 Iasi, Romania; vvulpe@uaiasi.ro (V.V.); spasca@uaiasi.ro (S.P.); drsupervet@gmail.com (M.C.); ionelabejan@gmail.com (I.S.); elena.gavrilas.dmv@gmail.com (E.G.)
- ⁵ Department of Mechanical Engineering, Faculty of Mechanics, “Gheorghe Asachi” Technical University Iasi, Mangeron Street, No. 29, 700050 Iasi, Romania; cornelmun@gmail.com (C.M.); bogdan.istrate@academic.tuiasi.ro (B.I.)
- ⁶ Department of Environmental Engineering and Management, Cristofor Simionescu Faculty of Chemical Engineering and Environmental Protection, “Gheorghe Asachi” Technical University of Iasi, 700050 Iasi, Romania; lbulg@ch.tuiasi.ro
- ⁷ Department of Plastic Surgery, “Grigore T. Popa”, University of Medicine and Pharmacy Iasi, Universitatii Street, No. 16, 700115 Iasi, Romania
- ⁸ Department of General Surgery, “Grigore T. Popa”, University of Medicine and Pharmacy Iasi, Universitatii Street, No. 16, 700115 Iasi, Romania
- * Correspondence: liliana.verestiuc@bioinginerie.ro (L.V.); camelia.tamas@umfiasi.ro (C.T.); Bogdan-mihnea.ciuntu@umfiasi.ro (B.M.C.)



Citation: Radu, C.D.; Verestiuc, L.; Ulea, E.; Lipsa, F.D.; Vulpe, V.; Munteanu, C.; Bulgariu, L.; Pașca, S.; Tamas, C.; Ciuntu, B.M.; et al. Evaluation of Keratin/Bacterial Cellulose Based Scaffolds as Potential Burned Wound Dressing. *Appl. Sci.* **2021**, *11*, 1995. <https://doi.org/10.3390/app11051995>

Academic Editor: Rossella Bedini

Received: 22 January 2021

Accepted: 18 February 2021

Published: 24 February 2021

Publisher's Note: MDPI stays neutral with regard to jurisdictional claims in published maps and institutional affiliations.



Copyright: © 2021 by the authors. Licensee MDPI, Basel, Switzerland. This article is an open access article distributed under the terms and conditions of the Creative Commons Attribution (CC BY) license (<https://creativecommons.org/licenses/by/4.0/>).

Abstract: The study presents the preparation and characterization of new scaffolds based on bacterial cellulose and keratin hydrogel which were seeded with adipose stem cells. The bacterial cellulose was obtained by developing an *Acetobacter xylinum* culture and was visualized using SEM (scanning electron microscopy) and elementally determined through EDAX (dispersive X-ray analysis) tests. Keratin species (β -keratose and γ -keratose) was extracted by hydrolytic degradation from non-dyed human hair. SEM, EDAX and conductometric titration tests were performed for physical-chemical and morphological evaluation. Cytocompatibility tests performed in vitro confirmed the material non-toxic effect on cells. The scaffolds, with and without stem cells, were grafted on the burned wounds on the rabbit's dorsal region and the grafts were monitored for 21 days after the application on the wounds. The clinical monitoring of the grafts and the histopathological examination demonstrated the regenerative potential of the bacterial cellulose-keratin scaffolds, under the test conditions.

Keywords: bacterial cellulose; keratin; stem cells; wound dressing; in vitro and in vivo tests

1. Introduction

Extensive and deep burn wounds represent a severe pathology, altering the general balance of the patient's status. Complex general and local therapy is required for the re-equilibration of the patients and recovering the protective barrier of the organism. Deep burns occupying over 15–20% from the body surface generate a multiple organ failure with progression to post-combustion shock. The time between the accident and the hospital

admission of the patient is critical for the future evolution. Any delay in providing the necessary care favors local and general complications and can lead to death [1].

Burned skin opens a huge gate for important loss of fluids, proteins, enzymes, electrolytes, altering the cardio-vascular, digestive, respiratory, and renal functions [2]. Increased blood viscosity generates a higher risk to thromboembolism and wound's bacterial invasion determines multiple organs failure and septic shock. Immediately after the injury, it is crucial to treat the pain, to restore the volume and hemodynamic balance, to correct the cellular hypoxia and prevent the main organs failure. It is equally important to excise the post burn necrosis and the challenge comes from the lack of donor zones sites, the high risk of wound deepening, and bacterial aggression [3,4]. Wound healing is a dynamic process that involves a complex series of events, lasting from the moment of injury to healing and includes increased activity of inflammatory, vascular, connective tissue, and epithelial cells. Wounds generally produce exudates that consist of fluids, cells or other substances that are slowly exuded or discharged from cells or blood vessels [5].

An important part of the clinical success is given by using a suitable biomaterial, with an appropriate mechanical resistance, which cover the wounds and prevent the fluid loss, the bacterial contamination, and stimulate the healing [6]. To cover and protect the burned wounds, usually sterile bandages are used. Recently, new possibilities were discovered such as artificial membranes for temporary wound protection. Another therapeutic solution is the use of autologous skin grafts, harvested from the patient's healthy skin donor zones. This last procedure has the main disadvantage that represents a new aggression for the skin areas and opens new gates for the bacterial invasion [7].

A useful biomaterial for burned wounds needs to respect the biocompatibility, to be able to stimulate the healing in a humid environment, to assure an efficiently antibacterial action without disturbing the biological cellular balance. Technically, a biomaterial offers the chance of biological reconstruction. It may be a scaffold, with a higher mechanical resistance, which functions like a support for skin cells. The cells will initiate the development of a keratinocytes film, which can be used to reconstruct the post burn defect [8,9].

Wound dressings have been fabricated starting from different types of materials and various formats, for example fiber mats and hydrogels, and may contain additives like silver or biological compounds for anti-bacterial properties [10]. Various natural or synthetic materials have been tested for wound healing purpose. Materials based on hyaluronan have been demonstrated to promote blood clotting and possess antibacterial properties [11–18]. Other polysaccharides, including alginates [19,20], chitosan [21–23], gelatin [24–26], and cellulose [27,28], have also been used to fabricate hydrogels for wound healing. Some synthetic polymers, like polyvinyl alcohol (PVA) [29,30], poly(ethylene glycol) (PEG), poly(acrylic acid) [31], and poly(lactic acid) [32] were tested and some of them presented antibacterial characteristics and as a hybrid with collagen, fibrin, or chitosan can promote wound regeneration [33–35].

Various hydrogels have been tested as wound dressings because of their similarity with extracellular matrices (ECM) [36]. The hydrogels are cell friendly environment and they represent an appropriate medium for proliferation, migration and differentiation of the cells. In order to improve the physical and mechanical properties of the polymeric hydrogels, while stimulating the healing process of the wounds, the hydrogels chemistry and morphology has been modified by using blends of natural and synthetic polymers, cross linkers, or drugs for preparing bioactive scaffolds and hydrogels [37–39].

Keratin-containing compounds have been tested, as a local therapeutic support for burned wounds, since ancient times. The choice of keratin as the second component of biomaterial is based on information from traditional Chinese medicine, which through millennial experience, has verified the therapeutic potential of using keratin as a remedy for burns. This, according to tradition, involves the removal of the hair from the patient, which, then, by burning, becomes an aseptic, opaque mass, of a dark color, and by grinding, a powder is obtained, based on keratin. The powder was deposited on the wound, the procedure being an archaic wound therapy, verified for about 2300 years in China [40]. Human

hair-derived keratin protein has been recognized as biomaterial with high potential due to its excellent bioactivity and biocompatibility and keratin-based hydrogels accelerated re-epithelization and wound healing process in a full-thickness tissue [41,42]. Recently, data about a new biomaterial obtained from bacterial cellulose (BC) and keratin, efficient for stimulating the wound repair and re-epithelialization were published [43,44].

In the surgical practice of burned wounds of large surface and depth, there is a severe deficiency of grafted skin. The paper offers an alternative to solve the issue. The aim of the study was to obtain a biomaterial from BC and keratin hydrogel, and to evaluate the effect of the cells inclusion (adipose stem cells) on the biological performances. The keratin component of the biomaterial directs the tissue development of stem cells to a grafting skin. Bacterial cellulose is the second component of the biomaterial being in the form of nanometric bundles and it offers the advantage of lack of chemical contaminants; as well, it reinforces scaffold for cell growth. CB allows obtaining a mechanically resistant biomaterial for wound grafting surgery. The result was a bio artificial material, later grafted on a burned wound. The grafted wound (in an in vivo study on rabbit), was monitored daily, both clinically and anatomic pathologically, and the biocompatibility was evaluated.

2. Materials and Methods

2.1. Materials

Bacterial pure strain *Komagataeibacter xylinum* (sin. *Acetobacter xylinum*, type strain DSM, no 6513), was purchased from Leibniz-Institut DSMZ (Braunschweig, Germany). Special bacterial culture media have been made in the Microbiology Laboratory using networks 105 (GOM) and 360 (YPM), from Leibniz-Institute DSMZ (Germany).

A mixture of solvents CHCl_3 , CH_3OH (96%) and H_2O_2 (32%) from Chimreactiv SRL, NaOH from S.C Atochim SRL were used for keratin hydrogel preparation.

For the cytocompatibility test have been used: primary stem cells from rabbit's adipose tissue; HBSS (buffer solution); sterile alcohol 70%; DMEM (special bacterial culture media); calf fetal serum (CFS); P/S/N (mixture of penicillin, streptomycin, neomycin); MTT (3-(4,5-dimethyl-2-tiazolyl)-2,5 diphenyl-2H-tetrazolium) bromide. All the reagents and solutions were purchased from Sigma-Aldrich (Steinheim, Germany).

For surgical proceeding the anesthesia some veterinary drugs were used: lidocaine infiltrations were performed for local anesthesia; for general anesthesia were used combinations of ketamine (35 mg/body weight), medetomidine hydrochloride (0.1 mg/body weight), butorphanol (0.5 mg/body weight).

2.2. Bacterial Cellulose (BC) Production

Pure bacterial culture of *Komagataeibacter xylinum* (sin. *Acetobacter xylinum*) where used for BC synthesis. Two special culture mediums were prepared: one in liquid form, for BC synthesis; another, in a solid form, for the bacterial species' conservation. The tested mediums were:

YPM (yeast peptone-mannitol extract): 5 g yeast extract; 3 g peptone; 25 g mannitol; 1000 mL distilled water; 12 g Agar is added to solidify the nutritious media.

GOM, nutritious media for *Gluconobacter oxydans*: 100 g glucose; 10 g yeast extract; 20 g CaCO_3 , 1000 mL distilled water; 15 g Agar is added to solidify the nutritious media.

Incorporation in liquid medium and the method of depletion of the handle on the surface of solid medium have been used as bacterial seeding techniques. After the liquid medium seeding with 1 mL suspension and the rotation of the culture Petri dishes for uniform inoculum distribution, they were placed in an incubator with constant temperature of 28 °C for 21 days. These are the conditions necessary to obtain a BC layer with a desired thickness. After testing the two culture mediums, the best results regarding the growth speed and the thickness of the BC layer were obtained on YPM. On this consideration, YPM was used for BC preparation in this study.

2.3. Obtaining the Keratin Hydrogel

The keratin hydrogel was prepared according to the Siller-Jackson et al. [45], with slightly modifications. Carefully selected undyed hair (origin from men, around 30 years old, provided by a hairdressing unit) was harvested, by cutting into segments of 2–5 cm length. The hair was grounded using a ball mill (Retsch PM 100, Retsch GmbH, Haan, Germany) at 100 rpm, for 30 min and transformed in pieces smaller than 1 mm; then, the samples were cleaned in a mixture $\text{CHCl}_3\text{-CH}_3\text{OH}$ (2:1; v/v) for 24 h at boiling point, using a Soxhlet extraction. The hair segments were then dried at 40 °C, for 24 h. Then, the hair was placed in distilled water, inside a stainless-steel sealed capsule, at a solid/liquid ratio = 2:35 (w/v). The capsule was maintained 2 h at 150 °C. After thermal treatment and cooling, the compound was centrifuged 10 min. at 10.000 rot/min. Two phases were separated: one solid, insoluble in water, considered a β -keratose, and one soluble in water, γ -keratose [46,47].

To prepare the β -keratose hydrogel, 2 g of solid phase were oxidized for 3 h, by boiling in a 3% H_2O_2 solution, with a liquor ratio of 1:11 (w/v). The solid compound obtained was cleaned in ethanol 96% and drained, by pressing with a filtering paper. The resulted solid was treated with 0.7% NaOH solution (in 70% ethanol), at a temperature of 70 °C. To keep the protein in a swollen state along the treatment, the pH was adjusted to 8. The compound was boiled for 3 h and then, maintained under stirring at 20 °C for 5 h. The product was filtered and washed with 100 mL distilled water; the purification was repeated 5 times.

The resultant β -keratose and γ -keratose were characterized by conductometric titration on the device pH/ion-center sensION MM 374 (Hach, Loveland, CO, USA).

2.4. Obtaining of Keratose-Bacterial Cellulose Scaffold

The bacterial cellulose membrane ($\phi = 6$ cm) was immersed in a solution of keratose (25 mL, 3%) for 24 h and a membrane with a gelatinous consistency was obtained by diffusion of the keratose, which was lyophilized and sterilized. For sterilization process, the materials were first exposed to UV radiation, one hour (30 min each part) and then were immersed in a sterile alcohol of 70%, for 30 min, cleaned with sterile distilled water (30 min) and immersed in HBSS (buffer solution) for 30 min. This procedure was repeated 3 times.

The last step consists of immersing the compound in culture media DMEM (4500 mg/L glucose, L-glutamine and liquid sodium bicarbonate, filtered under sterile conditions), three hours before the application in vivo.

2.5. Scaffolds Characterization

For the analysis of the composition and morphology, a Bruker QUANTA 200—3D DUAL BEAM EDS electron microscope was used with two systems (SEM and focused ion beam). By sending an electron beam on samples, images were obtained with different magnification degrees. EDAX dispersive X-ray analysis (EDX-VEGA II LSH//TESCAN instrument) was used to identify surface characteristics and high-resolution chemical analysis.

2.6. Cytocompatibility Tests and Cells Seeding

For the cytocompatibility assessment, the direct contact method was used. Adipose stem cells isolated from rabbit have been obtained using the protocol described by Bunnell et al. [48]. The cells were cultured in Dulbecco's modified eagle medium (DMEM) with 10% fetal bovine serum (FBS) and 1% penicillin-neomycin-streptomycin (P/N/S), in a humidified atmosphere of 5% CO_2 at 37 °C. When the cells reached sub-confluence, they were trypsinized with 0.25% trypsin containing 1 mM ethylenediamine tetra acetic acid (EDTA). The stem cells (5000 cells/well) were seeded on the culture media, using DMEM + 10% CFS (calf fetal serum) + 1% P/S/N (mixture of penicillin, streptomycin, neomycin), then incubated for 24 h (5% CO_2 , 37 °C). After the procedure, the culture medium was changed and the scaffolds were distributed in direct contact with the cells.

The MTT test was performed after 24, 48, and 72 h of direct contact between scaffolds and cells. For test, the culture medium was replaced with MTT solution 5% and incubated at 37 °C, 3 h. The viable cells reduce tetrazolium bromide-MTT in a colored compound, called formazan. The formazan was solubilized using isopropyl alcohol. The absorbance of formazan solution was spectrophotometrically measured at $\lambda = 570$ nm using a plate reader (Tecan Sunrise Plate Reader, Tecan Ltd., Männedorf, Switzerland). The spectrophotometrically reading results from the experimental wells were compared with the control wells (culture cells incubated with a same volume of PBS, with no materials included) and the cells viability was calculated with the following equation:

$$\text{Cell viability} = \frac{Abs_{sample}}{Abs_{control}} \times 100 \quad (\%) \quad (1)$$

where Abs_{sample} is the absorbance from the wells with scaffolds and $Abs_{control}$ is the absorbance in wells without scaffold.

In the aim to obtain cell seeded scaffold, a cell suspension (5000 cells, DMEM + 10% CFS medium) was incubated with scaffold ($\Phi = 6$ cm) for 48 h and used as obtained.

2.7. In Vivo Tests

For in vivo tests, 2 groups of rabbits (4 animal in each group) with a weight of 1–3.5 kg and an average age of 8 months, both sexes, were used. Rabbits of the common domestic breed were used. They were accommodated in individual cages from USAMV Biobase, Iasi; before the experiment, the animals had a period of accommodation of 7 days, while they were fed with vegetable food: cabbage, hay and carrots. The cycle light/darkness was respected. The tests on animals received the approval USAMV (University of Agricultural Science and Veterinary Medicine) Iasi, no 89/31st of January 2019 from the Ethics Commission concerning in vivo tests on animals.

Before experiment, a general anesthesia was performed, using a combination of ketamine (35 mg/body weight), medetomidine hydrochloride (0.1 mg/body weight) and butorphanol (0.5 mg/body weight). The local preparation included the hair cutting on a skin area of 3×3 cm, and a local asepsis using 100 mg/mL Povidone-iodine. To reduce the local post operative pain and inflammation, xylene infiltrations in four points, for local anesthesia were performed.

For each specimen, two burned wounds were performed: in the thoracic region, near the costal rim. L-shaped metallic device (3×3 cm) was used to produce the burned wounds. Heated to incandescent, the device was applied on the marked skin and maintained in direct contact for 4 s, without pressure. Then, one wound was grafted using a scaffold of BC and keratin hydrogel; another wound was covered with a scaffold containing BC, β -keratose hydrogel and stem cells from rabbit adipose tissue. The scaffolds were sutured in four points, for a better adhesion.

After the grafting procedure, the animals were monitored 3 weeks. Postoperatively, the animals were treated with antibiotic (enrofloxacin 0.5 mg/kg) for 3 days. The samples for the histological examination were collected in the days 7, 14, and 21. The clinical evaluation consisted in a general exam of the habit, skin and mucosa aspect before anesthesia, repeated postoperatively. The clinical daily monitoring was performed along the whole duration of the experiment. No change in the physiology of the 8 animals was noted.

2.8. Histopathological Analysis

Samples collection, from the tissue areas of interest of the lots marked with C (control lot), K + cel (keratin and bacterial cellulose hydrogel) and K + cel + S (keratin and bacterial cellulose hydrogel seeded with stem cells) was performed in the days 7, 14, and 21 from the beginning of the experiment. Small tissue biopsies (6 mm, KRUUSE Biopsy punch sterile) were collected from the wounds' borders and fixed in 10% buffered formaldehyde for 48 h. Then, the samples were processed by the method of inclusion in paraffin (processor Leica TP 1020—Germany) and divided in pieces with 5 μ m thickness. The pieces were colored

trichomic Masson and examined with a Leica DM 1000 photonic microscope. A Leica 5 mpx full HD digital histological camera was used for image capturing, alongside LAS software, version 2016.

3. Results and Discussion

3.1. BC and Keratose Preparation

The synthesis of cellulose by *Komagataeibacter xylinum* is carried out by polymerization and crystallization, both enzymatic catalysts [47,49]. The authors reported that a *Komagataeibacter xylinum* cell (Gram-negative, aerobic, and cylindrical bacterium) produces BC, as a result of acetic acid fermentation, developing a polymerization rate of 200,000 glucose molecules/second. Nanometric size of cellulose filaments, good mechanical strength and chemical purity determine the selection of bacterial cellulose that can be constituted from the biomaterial point of view.

Bacteria synthesize cellulose because it retains a high amount of moisture, which prevents dehydration of the bacterium, ensuring its vitality for a long period of time. Further, cellulose captures the carbon dioxide molecules resulting from cellulose synthesis, ensuring the bacteria float on the surface of the water, thus having easy access to oxygen in the air; being aerobic, this means good nutrition at the interface with atmospheric air. Due to its opaque nature, cellulose film protects the bacteria from the destructive and dangerous effect of UV radiation [49]. Alternatively, by developing cellulose in water, a barrier is formed that inhibits colonization of the environment by other bacteria which discourages unwanted competition with the host bacterium.

The obtained biomaterial consists of BC in the form of a nanofibrils and keratin veil. The procedure involves avoiding the rejection of keratin by the patient's immune system as a foreign body reaction; respectively the burning of keratin achieves the condition of sterility.

By treating with water at 150 °C, inside the capsule, a pressure of 4.9 atmospheres (about 48,10⁴ Pa) is developed [50], which determines the hydrolytic degradation of keratin. After this process, β-keratose and γ-keratose are obtained. β-keratose contains high molecular weight proteins, with disulfide cross-linkages which determine its insolubility. This fraction may also contain partially oxidized peptide chains or peptides with a percentage of splinted disulfide bonds. This structure facilitates obtaining of the β-keratose hydrogel. The second fraction, γ-keratose, consists of fragments oxidized keratin and cleaved into small molecules, usually cysteine derivatives. β-keratose hydrogel and partially a γ-keratose solution were used in this study.

It has been found that γ-keratose obtained by hydrolysis of human hair has acidic pH. For the qualitative evaluation of the protein composition and dispersion of the γ-keratin, a conductometric titration with NaOH was performed. The titration curve (triplicates) is illustrated in Figure 1.

It can be observed four domains with molecular fractions. According to the equivalence formula, the calculated normality for each domain is

$$N_{1\text{strong acids}} \times \text{Sample volume} = N \text{ NaOH} \times V_{\text{eq1}} \quad (2)$$

where N_1 strong acids represents the normality of part 1 components (equiv./liter); N NaOH is the normality of the sodium hydroxide solution used in the titration (0.1 in this case); V_{eq1} = the graphically determined volume of equivalence in domain 1 (mL) illustrated.

From Formula (2), the number of strong acid equivalents is calculated:

$$N_{1\text{strong acids}} = (N \text{ NaOH} \times V_{\text{eq1}}) / \text{Sample volume} \quad (3)$$

Similarly, for the other domains respectively, the range 2 between pH = 0.75–1.7, the range 3 between 1.7 and 3.2 and the range 4 between 3.2 and 4.8 were obtained. Table 1 shows the values of equivalents/liter number obtained on the four domains.

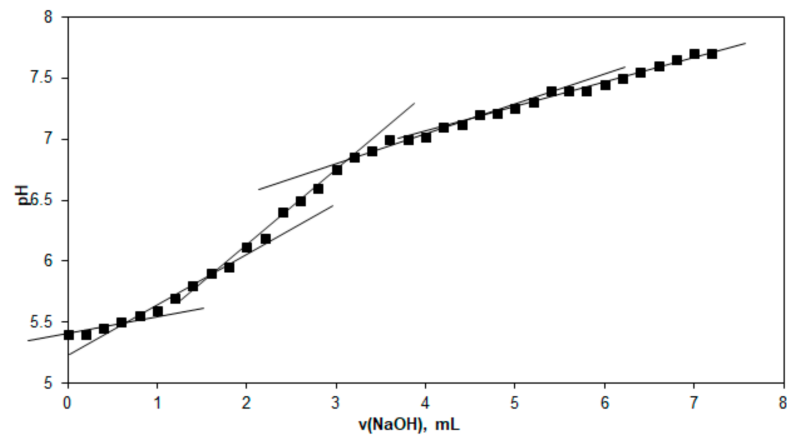


Figure 1. Conductometric titration curve of γ -keratose solution.

Table 1. Acid equivalents from γ -keratose calculation.

No.	Domain	Equivalence Volume (mL)	Sample Volume (mL)	Equivalents/Liter
1	1	0.75	10	0.0075
2	2	1.70	10	0.0170
3	3	3.20	10	0.0320
4	4	4.80	10	0.0480

Table 1 illustrates the values of the acid equivalents on the domains obtained by conductometric titration of γ -keratose solution, after the hydrolytic degradation treatment. These are sulfonic or other acid derivatives reaction, obtained following the keratin macromolecular chain breaks, due to the hair hydrolytic treatment, at 150 °C and 4.9 atm. According to the literature [51,52] it is considered that in domain 1 Table 1 the protein fraction has a strong acid behavior (sulfonic group), in domain 2 there are less acidic proteins, possibly acids carboxylic acids with high molecular weight, low molecular weight alcohols or aromatic alcohols having a resonance effect with increasing acidity (hydrogen atom lability). In domain 3 there are sterically hindered aliphatic alcohols. Domain 4 is characterized by the excess of NaOH that is usually identified by titration. Figure 2 illustrates schematically the hypothetical chemical transformations.

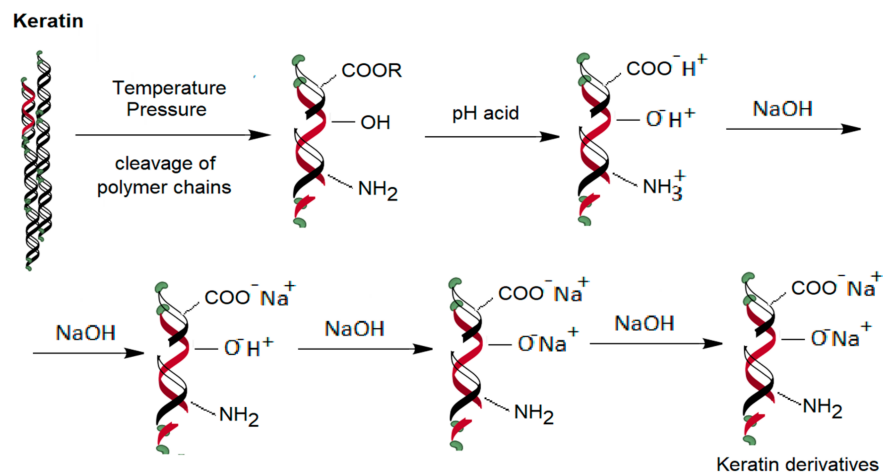


Figure 2. Schematic reaction to obtain the carboxylic derivatives, highlighted conductometrically.

Obtaining groups of protein fragments with sulfonic components is done by splitting the disulfide bond of the cysteine according to the reaction illustrated in Figure 3.

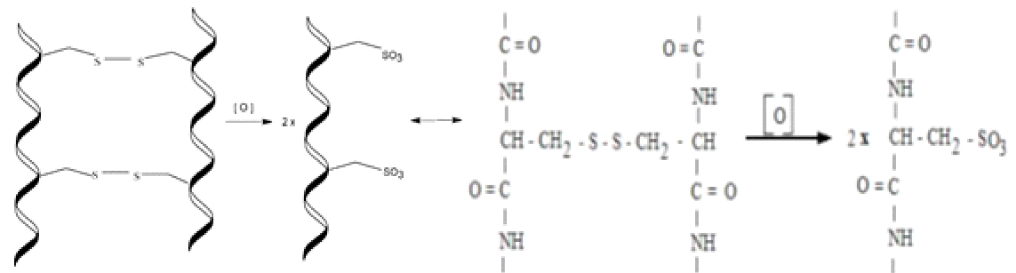


Figure 3. Splitting reaction of disulfide bond from keratin oxidation to sulfonic groups.

The potentiometric curve of beta-keratose hydrogel is illustrated in Figure 4. The curve consists of three straight segments, one red and other two blue having two points of intersection (volumes of equivalence).

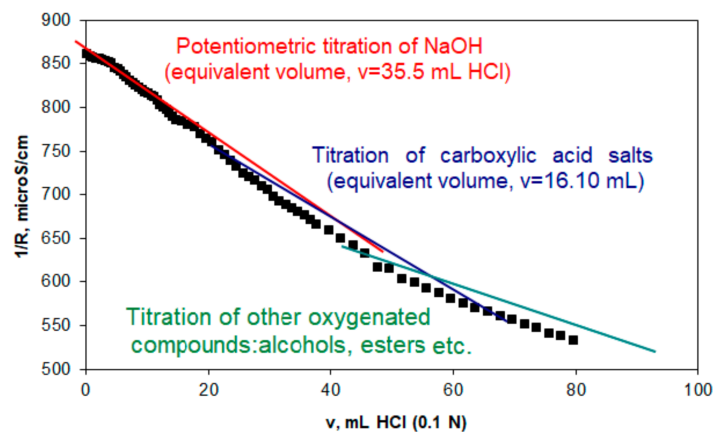
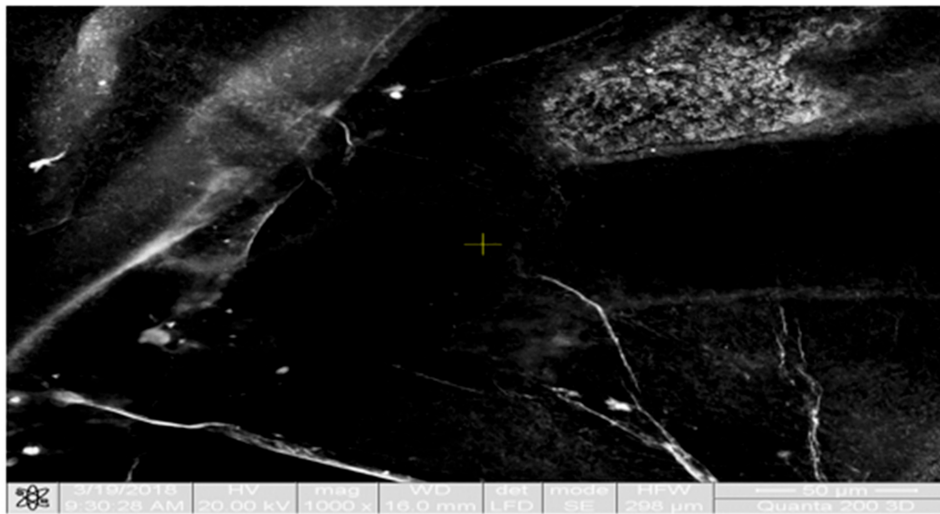


Figure 4. The potentiometric titration of β -keratose hydrogel.

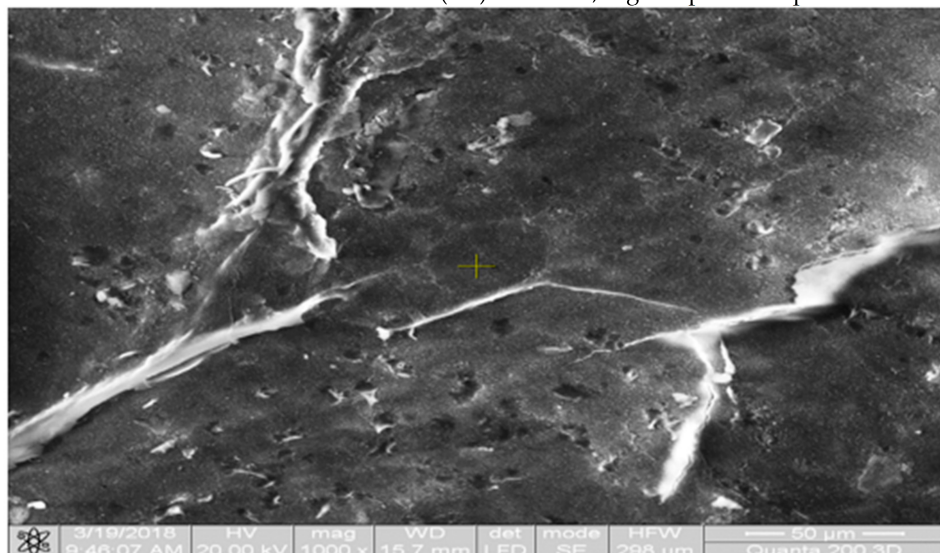
The red curve is the titration of the excess of NaOH (present on obtaining the hydrogel) up to the first volume of equivalence. The second line segment is the second equivalence volume. From here to increasing values the titration of salts of other oxygenated compounds (alcohols, esters, etc.) begins.

3.2. Scaffolds Morphology

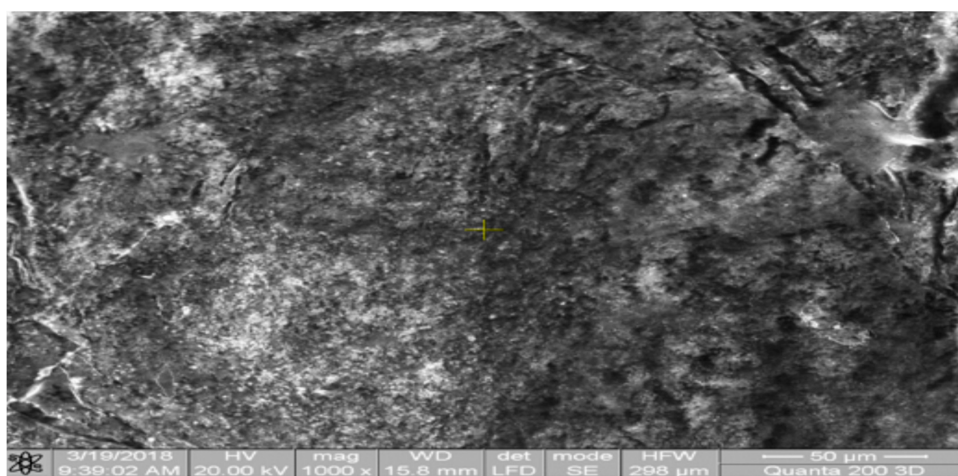
Through bacterial growth, a gelatinous mass was obtained in the form of a nanometric veil of BC filaments without any chemical contaminants. Figure 5a illustrates the microphotography of lyophilized BC film, Figure 5b the microphotography of the BC— β -keratose scaffold and, respectively, Figure 5c the microphotography of BC— γ -keratose scaffold.



(a) Black dots = bundles of bacterial cellulose (BC) filaments; Lighter points dispersed BC in water.



(b) Black dots = bundles of BC filaments; Grey points dispersed β -keratose.



(c) Black dots = bundles of BC filaments; Grey points dispersed- γ -keratose.

Figure 5. (a) A SEM microphotography of the BC scaffold. (b) SEM microphotography of the BC- β -keratose scaffold. (c) SEM microphotography of the BC- γ -keratose scaffold.

The BC scaffold present relatively homogeneous portions of scattered BC filaments (black dots) that probably visualize sections of the nanofiber bundles located in a quasi-uniform environment, delimited on portions by separation fissures, as can noticed in Figure 5a.

As can be seen in Figure 5b, the BC- β -keratose scaffold presents both components of the biomaterial, BC and the keratinous part, organized in form of dark colored islands, probably BC bundles dispersed in a homogeneous environment of gray keratin hydrogel. The same type of organization is observed, in the form of dark zones delimited by continues white fissures.

In the Figure 5c above the BC- γ -keratose SEM image revealed a more homogeneous organization. The γ -keratose (the soluble component resulting from the hair hydrolysis) is observed on large portions, as a light dispersion medium. The material contains small molecular weight keratin fragments and favors their dispersion. The dark-colored of BC bundles appear as dots shape.

3.3. EDAX Elemental Analysis

Figure 6 and Table 2 below demonstrate that the BC biomass and keratose solution have the characteristic elements of protein chains: C, O, and N, and S as a specific element in the disulfide of cysteine fragments, possibly fragments with sulfonic functional groups, explaining the solubility of gamma-keratose compared to the insoluble portion of beta-keratose resulting from hydrolytic cleavage. The analysis of the biomaterial consisting of the keratose range containing small molecular weight fragments and cysteine fragments with high frequency of sulfonic groups was chosen.

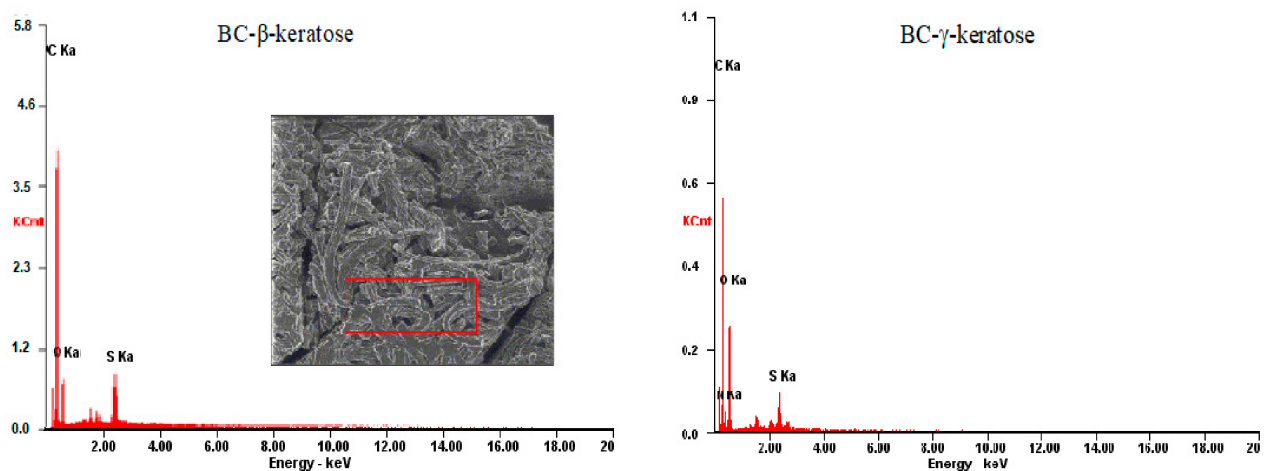


Figure 6. EDAX elemental analysis of the BC-keratose scaffolds.

Table 2. Elemental weight value for BC-keratose scaffolds.

No.	BC- β -Keratose			BC- γ -Keratose		
	Element	Wt %	At %	Element	Wt %	At %
	C	65.01	73.29	C	50.75	58.78
	N	02.10	02.04	N	02.98	02.96
	O	25.70	21.65	O	41.75	36.30
	S	07.19	03.02	S	04.51	01.96
	Matrix	Correction	ZAF	Matrix	Correction	ZAF

Wt (%), the percentage mass of the element, At (%), the percentage composition of the atomic weight.

3.4. Cytocompatibility Tests

An important aim of the wound dressing's material is to achieve an appropriate and efficient way for soft tissue regeneration which often consists of a large compartment of the

cells-rich medium. Figure 7 illustrates the results obtained on bacterial cellulose (BC) and BC-keratose scaffolds, all seeded with stem cells. The relative metabolic activity induced by the scaffolds was over 95% and dependent of the scaffold composition.

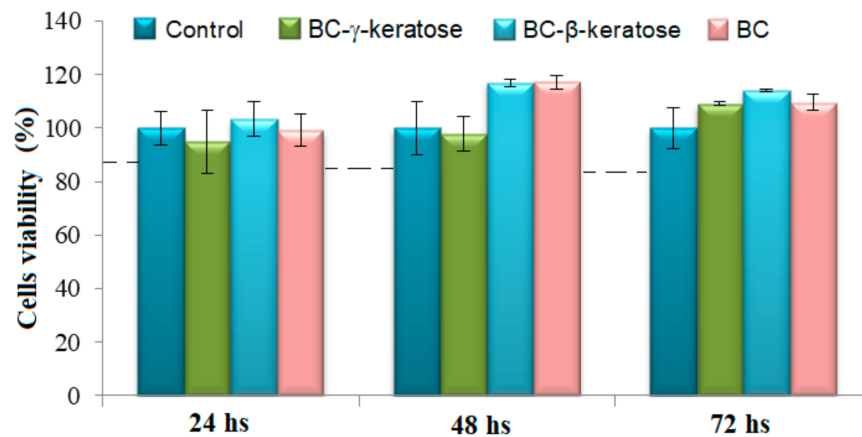


Figure 7. Cell viability data for BC-keratose scaffolds (MTT assay at 24 h, 48 h, and 72 h).

Cell viability tests show that after 48 and 72 h, respectively, from seeding, on BC and BC- β -keratose an increase in the number of cells until comparing with control culture. The cell viability increased over 115%, indicating an effect of stimulation of cells growths and differentiation. A similar effect, but less intensive was observed for BC- γ -keratose. The result could be determined by a better distribution the β -keratose in the BC membrane because of their supramolecular structure. The data of cytotoxicity on the obtained materials are in agreement with other authors' results about BC cellulose stimulating effect on cells activity [53].

3.5. In Vivo Tests

For the clinical testing of the scaffolds, eight common breed rabbits were included. A general clinical examination was performed before anesthesia and included the assessment of the habitus, skin and mucous membranes, the examination being repeated and post-intervention. The results also depend on various co-morbidities, in multicellular organisms, both health and disease are defined by means of communication patterns involving the component cells. Clinical supervision was performed daily throughout the experiment; no changes in the physiological state were reported in the rabbits included in the study [54–57]. The appearance of the wound was followed and a favorable evolution was observed after the graft. One noticed the obvious recurrence of hairs throughout the wound contour, the absence of inflammation, and after taking biological samples for anatomic–pathological tests, the revascularization of the tissue [4,58]. Palpation of the area shows a hard, normal appearance, without a painful sensation. The evolution of wound recovery is presented in the next images (Figure 8), where, M is the wound grafted with biomaterial made of BC- β -keratose and X wound grafted with biomaterial of BC- β -keratose and artificial tegument.

Histopathological evaluation was carried out on the marginal areas of wounds, in all experimental groups. The morphology of the local inflammation, the conjunctive-vascular buds' formation and the epidermis regeneration process were monitored.

At seven days after grafting the histopathological exam (after the established criteria) did not reveal any significant differences between the animal groups (Figure 9). All the studied animals developed increased dermo-epidermal coagulation necrosis, inflammatory infiltration in the hypoderm, represented by neutrophilic leukocytes, histiocytes and macrophages, all implicated in necrotic tissue detorsion. A congestion of the blood capillaries and a pronounced local edema, with the dissociation of local structural elements, was observed in the hypoderm.

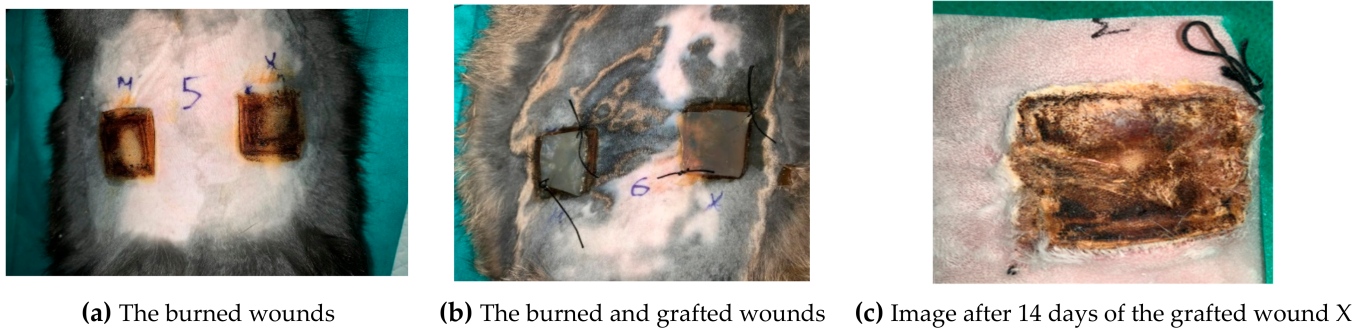


Figure 8. (a) illustrates the appearance of the two burned wounds A and X both covered with a dressing; (b) one illustrated the case of the burned wounds already grafted as one mentioned above. (c) is the appearance of grafted wound after an evolution of 14 days from the grafting date. One notices the appearance of hairs grown in the area of the grafted wound compared to the dorsal area of the rabbit previously cut for clinical study.

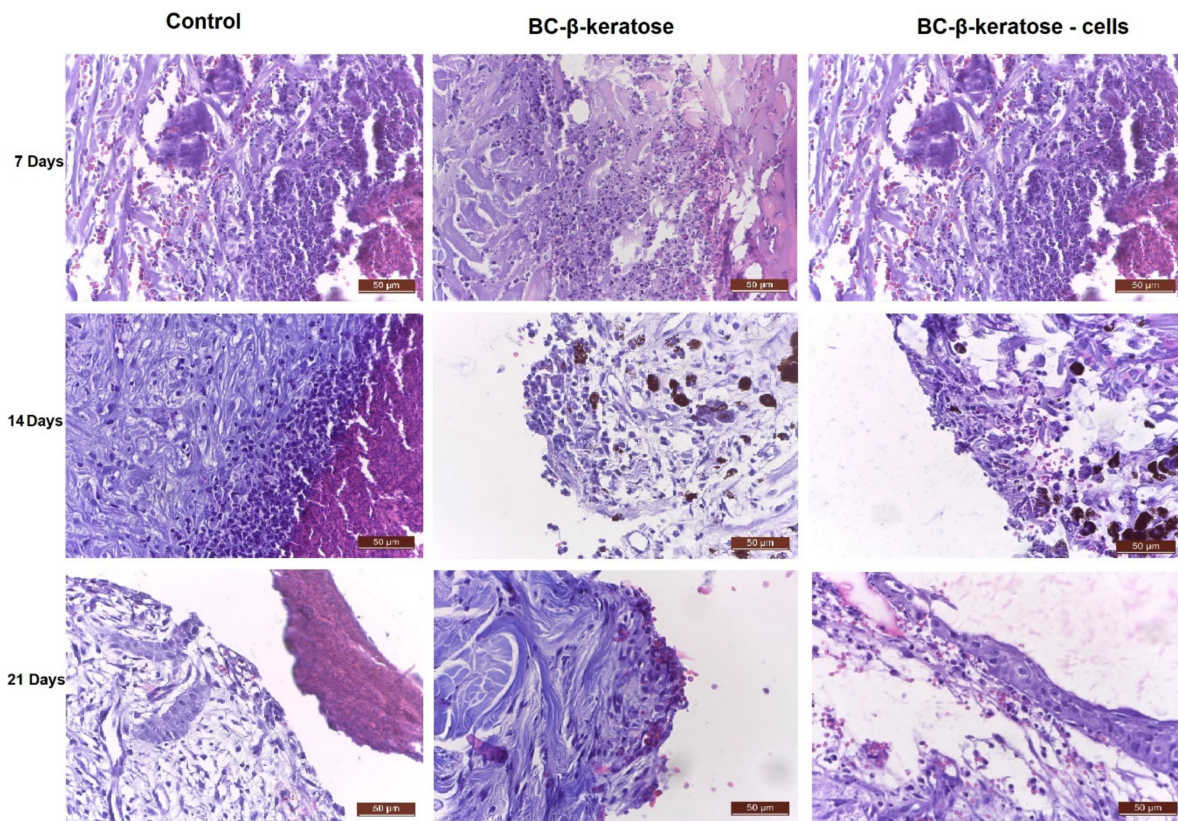


Figure 9. Microscopic images of the stained histological sections (trichrome Masson staining) made on the tissues at different times after grafting (7 days, 14 days, 21 days).

At 14 days after grafting, the sections from control group revealed an inflammatory process which slightly decreases in intensity. The influx of leukocytes was maintained. A discreet fibroblasts differentiation, connective fibers and blood vessels neogenesis were observed in hypoderm. Animals tissues grafted with BC- β -keratose developed an inflammatory process with lower intensity. The healing process is represented by important connective hyperplasia and neogenesis of blood vessels, with the formation of prominent vascular-conjunctive buds. At lot BC- β -keratose with cells, the inflammatory process is discreet; the regeneration is markedly, represented by vascular, connective buds, and fibroblast proliferation. Connective fibers and capillary neogenesis are important.

At 21 days after grafting at the animals from control group the inflammatory process is considerably reduced and the skin regeneration is represented by young conjunctive and vascular buds. The buds are covered with a superficial condensed cellular layer, without a basal membrane, suggesting a future stratified young and plane epithelium cells. Animals grafted with BC- β -keratose indicated that the re-epithelialization process is more advanced. On the surface of the connective bud, a young, unorganized, and untargeted epithelium is observed, consisting of slightly flattened skin cells. On the wounds from the animals grafted with BC- β -keratose and cells, an important epidermal regeneration was noted. A young, pavements epithelium, with a well-represented basal lamina and 2–3 rows of more or less flattened epithelial cells were present.

3.6. Histopathological Results Interpretation

Inflammatory and regenerative processes for the main skin structures (hypoderm, dermis, and epidermis) were followed by histological examination. The samples were harvested from the periphery of the lesions, at the border with the unaffected tissue. The degree of proliferation and differentiation of local and migrated cells, neogenesis of connective fibers and blood capillaries, regeneration of the keratinized epidermal pavement epithelium where appreciated.

At seven days post grafting the inflammatory process was similar to the three groups of experimental animals (Control, BC- β -keratose, BC- β -keratose-cells). No significant differences in the evolution of the inflammatory process and the healing process were observed.

At 14 days post grafting the predominance of the inflammatory exudate was observed in Control group, unlike the other two batches, where the regeneration process was already initiated, well outlined. At the dermis level, vascular-conjunctives buds, constituted by fibroblast differentiation, young connective tissue and marked neoangiogenic were observed. It has also been noticed, in both experimental batches (BC- β -keratose, BC- β -keratose-cells), intensive detorsion process of necrotic areas.

At 21 days post grafting evaluation dermis regeneration was more intense and rapid at (BC- β -keratose) and (BC- β -keratose-cells), comparing with extremely low levels in Control group. Dermal regeneration in the Control-group consisted of conjunctive-vascular papilla formation, fibroblast proliferation, collagen fibers synthesis, and angiogenesis. On the surface of the papilla was noted a cellular condensation suggesting the onset of epidermal regeneration, but without a proper basal lamina.

Epidermis regeneration was quantified by evaluating the epithelialization, the formation of the basal lamina and the basal layer, with its proliferation and the restoration of the stratified keratinized pavements epithelium as shown in Table 3.

The regeneration of the epidermis was much more evident in the BC- β -keratose-cells group compared to the BC- β -keratose one. Young, stratified epithelium, undergoing reshuffle and evolution towards keratinocytes, represented by basal lamina and 2–3 layers of epithelial cells were noticed.

Following the results, we concluded that skin regeneration was much faster in BC- β -keratose and BC- β -keratose-cells batches, especially during the last two weeks of the experiment. The process of scarring, with the elimination of necrotic detriment and reconstruction of damaged structures by the action of the heat agent, was carried out much faster in experimental batches than at the control lot. This demonstrates the important role of keratin material and cellulose in the formation of a mechanical barrier with protection function.

This barrier represents, also, a support for the cells involved in necrosis detorsion and tissular regeneration. In addition, in BC- β -keratose-cells group the higher capacity of skin regeneration was justified by stem cells activity. Stem cells differentiation and proliferation contribute, alongside local and immigrant cells, to the restoring process of affected structures.

Table 3. Anatomic–pathological results.

Healing Parameters	Control	BC-β-Keratose	BC-β-Keratose-Cells
7 days post grafting			
Inflammation	++++	++++	++++
Dermis regeneration (fibroblasts, connective tissue, vascular neogenesis)	-	-	-
Epidermal regeneration	-	-	-
14 days post grafting			
Inflammation	+++	++	+
Dermis regeneration (fibroblasts, connective tissue, vascular neogenesis)– connective -vascular bud	+	++	+++
Epidermis regeneration	-	-	-
21 days post grafting			
Inflammation	+	-	-
Dermis regeneration (fibroblasts, connective tissue, vascular neogenesis)	++	+++	++++
Epidermis regeneration	+	++	+++

Legend: “+”–very low grade of epithelization; “++”–low grade of epithelization; “+++”–intermediate grade of epithelization; “++++”–high grade of epithelization; “-”–absence of epithelization.

4. Conclusions

Scaffolds based on bacterial cellulose (as a result of the *Komagataeibacter xylinum* bacterial species activity) and keratin derivates were obtained and tested. The scaffolds have been seeded with stem cells isolated from the rabbit’s adipose tissue. The stem cells have initiated tissular growth with an appropriate viability. The composite biomaterials were grafted on the burned wounds on rabbits of the common breed. The treated wounds presented a favorable evolution. The process of scarring, with the necrotic tissue detersion and reconstruction of damaged structures by the action of the heat agent, was carried out much faster in comparison with control, which demonstrates the important role of keratin, cellulose and stem cells. Cellulose and keratin played the role of an important barrier, with protection and support activities for the cells involved in detersion and regeneration. The stem cells, by differentiation, contributed alongside local and immigrant elements to the restoration process of the affected structures.

Author Contributions: Conceptualization and project administration C.D.R., investigation and data curation L.V. and C.V.M., methodology and supervision C.D.R. and C.M., methodology and investigation S.P., E.G., C.T., B.M.C., M.C., formal analysis and investigation E.U., V.V., B.M.C., L.B., F.D.L., C.T., I.S., C.V.M., and B.I., writing—review and editing and validation C.D.R. and C.M. All authors have read and agreed to the published version of the manuscript.

Funding: The work did not use financial resources involving any company or institution.

Institutional Review Board Statement: The study was conducted according to the guidelines of the Declaration of Helsinki, and the tests on animals received the approval USAMV (University of Agricultural Science and Veterinary Medicine) Iasi, no 89/31st of January 2019 from the Ethics Commission concerning in vivo tests on animals.

Informed Consent Statement: Not applicable.

Data Availability Statement: Data sharing not applicable.

Conflicts of Interest: The authors declare no conflict of interest.

References

1. Arbuthnot, M.K.; Garcia, A.V. Early resuscitation and management of severe pediatric burns. *Semin. Pediatr. Surg.* **2019**, *28*, 73–78. [[CrossRef](#)] [[PubMed](#)]
2. McLaughlin, E.S.; Paterson, A.O. (Eds). *Burns: Prevention, Causes and Treatment*; First Chapter; Nova Publishers: Hauppauge, NY, USA, 2012; pp. 31–37.
3. Clark, A.; Imran, J.; Madni, T.; Wolf, S.E. Nutrition and metabolism in burn patients. *Burn. Trauma* **2017**, *5*, 11. [[CrossRef](#)] [[PubMed](#)]
4. Barrett, L.W.; Fear, V.S.; Waithman, J.C.; Wood, F.M.; Fear, M.W. Understanding acute burn injury as a chronic disease. *Burn. Trauma* **2019**, *7*, 23. [[CrossRef](#)] [[PubMed](#)]
5. Singh, B.; Sharma, S.; Dhiman, A. Design of antibiotic containing hydrogel wound dressings: Biomedical properties and histological study of wound healing. *Int. J. Pharm.* **2013**, *457*, 82–91. [[CrossRef](#)]
6. Sorg, H.; Tilkorn, D.J.; Hager, S.; Hauser, J.; Mirastschijski, U. Skin Wound Healing: An Update on the Current Knowledge and Concepts. *Eur. Surg. Res.* **2017**, *58*, 81–94. [[CrossRef](#)]
7. Augustine, R.; Kalarikkal, N.; Thomas, S. Advancement of wound care from grafts to bioengineered smart skin substitutes. *Prog. Biomater.* **2014**, *3*, 103–113. [[CrossRef](#)]
8. Mir, M.; Ali, M.N.; Barakullah, A.; Gulzar, A.; Arshad, M.; Fatima, S.; Asad, M. Synthetic polymeric biomaterials for wound healing: A review. *Prog. Biomater.* **2018**, *7*, 1–21. [[CrossRef](#)] [[PubMed](#)]
9. Chouhan, D.; Mandal, B.B. Silk biomaterials in wound healing and skin regeneration therapeutics: From bench to bedside. *Acta Biomater.* **2020**, *103*, 24–51. [[CrossRef](#)] [[PubMed](#)]
10. Murray, R.Z.; West, Z.E.; Cowin, A.J.; Farrugia, B.L. Development and use of biomaterials as wound healing therapies. *Burn. Trauma* **2019**, *7*, 2. [[CrossRef](#)] [[PubMed](#)]
11. Zhu, J.; Li, F.; Wang, X.; Yu, J.; Wu, D. Hyaluronic Acid and Polyethylene Glycol Hybrid Hydrogel Encapsulating Nanogel with Hemostasis and Sustainable Antibacterial Property for Wound Healing. *ACS Appl. Mater. Interfaces* **2018**, *10*, 13304–13316. [[CrossRef](#)] [[PubMed](#)]
12. Liyang, S.; Yannan, Z.; Qifan, X.; Caixia, F.; Jöns, H.; Jianwu, D. Moldable hyaluronan hydrogel enabled by dynamic metal–bisphosphonate coordination chemistry for wound healing. *Adv. Healthc. Mater.* **2018**, *7*, 1700973.
13. Neuman, M.G.; Nanau, R.M.; Oruña-Sánchez, L.; Coto, G. Hyaluronic Acid and Wound Healing. *J. Pharm. Pharm. Sci.* **2015**, *18*, 53–60. [[CrossRef](#)] [[PubMed](#)]
14. Longinotti, C. The use of hyaluronic acid based dressings to treat burns: A review. *Burn. Trauma* **2014**, *2*, 162–168. [[CrossRef](#)] [[PubMed](#)]
15. Botnariu, G.; Popa, A.; Mitrea, G.; Manole, M.; Pacurar, M.; Anghele, M.; Curis, C.; Teodorescu, E. Correlation of Glycemic and Lipid Control Parameters with Cognitive Dysfunction Scores, in Type 2 Diabetic Persons Results from a cross-sectional study. *Rev. Chim.* **2019**, *69*, 3486–3489. [[CrossRef](#)]
16. Botezatu, C.; Duceac, L.D.; Mastalier, B.; Stafie, L.; Jitareanu, C.M.; Luca, A.C.; Tarca, E.; Mitrea, G.; Iordache, A.C.; Patrascu, T. Hepatic Cystic Echinococcosis Studied in A Family Group. *IJMD* **2018**, *22*, 346–350.
17. Ichim, D.L.; Duceac, L.D.; Marcu, C.; Iordache, A.C.; Ciomaga, I.M.; Luca, A.C.; Goroftei, E.R.B.; Mitrea, G.; Damir, D.; Stafie, L. Synthesis and Characterization of Colistin Loaded Nanoparticles Used to Combat Multi-drug Resistant Microorganisms. *Rev. Chim.* **2019**, *70*, 3734–3737. [[CrossRef](#)]
18. Luca, A.C.; Eva, L.; Iordache, A.C.; Duceac, L.D.; Mitrea, G.; Marcu, C.; Stafie, L.; Ciuhodaru, M.I.; Ciomaga, I.M.; Goroftei, E.R.B.; et al. Drug Encapsulated Nanomaterials as Carriers Used in Cardiology Field. *Rev. Chim.* **2020**, *71*, 413–417. [[CrossRef](#)]
19. Aderibigbe, B.A.; Buyana, B. Alginate in Wound Dressings. *Pharmaceutics* **2018**, *10*, 42. [[CrossRef](#)]
20. Wang, T.; Gu, Q.; Zhao, J.; Mei, J.; Shao, M.; Pan, Y.; Zhang, J.; Wu, H.; Zhang, Z.; Liu, F. Calcium alginate enhances wound healing by up-regulating the ratio of collagen types I/III in diabetic rats. *Int. J. Clin. Exp. Pathol.* **2015**, *8*, 6636–6645.
21. Liu, H.; Wang, C.; Li, C.; Qin, Y.; Wang, Z.; Yang, F.; Li, Z.; Wang, J. A functional chitosan-based hydrogel as a wound dressing and drug delivery system in the treatment of wound healing. *RSC Adv.* **2018**, *8*, 7533–7549. [[CrossRef](#)]
22. Ahmed, S.; Ikram, S. Chitosan Based Scaffolds and Their Applications in Wound Healing. *Achiev. Life Sci.* **2016**, *10*, 27–37. [[CrossRef](#)]
23. Patrulea, V.; Ostafe, V.; Borchard, G.; Jordan, O. Chitosan as a starting material for wound healing applications. *Eur. J. Pharm. Biopharm.* **2015**, *97*, 417–426. [[CrossRef](#)] [[PubMed](#)]
24. Acevedo, C.A.; Sánchez, E.; Orellana, N.; Morales, P.; Olguín, Y.; Brown, D.I.; Enrione, J. Re-Epithelialization Appraisal of Skin Wound in a Porcine Model Using a Salmon-Gelatin Based Biomaterial as Wound Dressing. *Pharmaceutics* **2019**, *11*, 196. [[CrossRef](#)] [[PubMed](#)]
25. Jang, H.-J.; Kim, Y.-M.; Yoo, B.-Y.; Seo, Y.-K. Wound-healing effects of human dermal components with gelatin dressing. *J. Biomater. Appl.* **2018**, *32*, 716–724. [[CrossRef](#)] [[PubMed](#)]
26. Zheng, Y.; Liang, Y.; Zhang, D.; Sun, X.; Liang, L.; Li, J.; Liu, Y.N. Gelatin-Based Hydrogels Blended with Gellan as an Inject-able Wound Dressing. *ACS Omega* **2018**, *3*, 4766–4775. [[CrossRef](#)]

27. Kiiskinen, J.; Merivaara, A.; Hakkarainen, T.; Kääriäinen, M.; Miettinen, S.; MarjoYliperttula, M.; Koivuniemi, R. Nano-fibrillar cellulose wound dressing supports the growth and characteristics of human mesenchymal stem/stromal cells without cell adhesion coatings. *Stem. Cell Res. Ther.* **2019**, *10*, 292. [[CrossRef](#)] [[PubMed](#)]
28. Savitskaya, I.S.; Shokatayeva, D.H.; Kistaubayeva, A.S.; Ignatova, L.V.; Digel, I.E. Antimicrobial and wound healing properties of a bacterial cellulose based material containing *B. subtilis* cells. *Helion* **2019**, *5*, e02592. [[CrossRef](#)] [[PubMed](#)]
29. Gao, T.; Jiang, M.; Liu, X.; You, G.; Wang, W.; Sun, Z.; Ma, A.; Chen, J. Patterned Polyvinyl Alcohol Hydrogel Dressings with Stem Cells Seeded for Wound Healing. *Polymers* **2019**, *11*, 171. [[CrossRef](#)]
30. Hikmawati, D.; Rohmadanik, A.R.; Putra, A.P.; Siswanto, A. The Effect of Aloe vera Extract Variation in Electrospun Polyvinyl Alcohol (PVA)-Aloe vera-Based Nanofiber Membrane. *J. Phys. Conf. Ser.* **2018**, *1120*, 012096. [[CrossRef](#)]
31. Champeau, M.; Póvo, V.; Militão, L.; Cabrini, F.M.; Picheth, G.F.; Meneau, F.; Jara, C.P.; de Araujo, E.P.; de Oliveira, M.G. Supramolecular poly(acrylic acid)/F127 hydrogel with hydration-controlled nitric oxide release for enhancing wound healing. *Acta Biomater.* **2018**, *74*, 312–325. [[CrossRef](#)]
32. Nguyen, T.T.T.; Ghosh, C.; Hwang, S.-G.; Tran, L.D.; Park, J.S. Characteristics of curcumin-loaded poly (lactic acid) nanofibers for wound healing. *J. Mater. Sci.* **2013**, *48*, 7125–7133. [[CrossRef](#)]
33. Foong, C.Y.; Hamzah, M.S.A.; Razak, S.I.A. Influence of Poly(lactic acid) Layer on the Physical and Antibacterial Properties of Dry Bacterial Cellulose Sheet for Potential Acute Wound Healing Materials. *Fibers Polym.* **2018**, *19*, 263–271. [[CrossRef](#)]
34. Napavichayanun, S.; Bonani, W.; YYang, Y.; Motta, A.; Aramwit, P. Fibroin and Polyvinyl Alcohol Hydrogel Wound Dressing Containing Silk Sericin Prepared Using High-Pressure Carbon Dioxide. *Adv. Wound Care* **2019**, *8*, 452–462. [[CrossRef](#)]
35. Lin, S.-P.; Lo, K.-Y.; Tseng, T.-N.; Liu, J.-M.; Shih, T.-Y.; Cheng, K.-C. Evaluation of PVA/dextran/chitosan hydrogel for wound dressing. *Cell. Polym.* **2019**, *38*, 15–30. [[CrossRef](#)]
36. Zhu, J.; Marchant, R. Design properties of hydrogel tissue-engineering scaffolds. *Expert Rev. Med. Devices* **2011**, *8*, 607–626. [[CrossRef](#)]
37. Perez, R.A.; Kim, M.; Kim, T.H.; Kim, J.H.; Lee, J.H.; Park, J.H.; Knowles, J.C.; Kim, H.W. Utilizing core-shell fibrous collagen-alginate hydrogel cell delivery system for bone tissue engineering. *Tissue Eng.* **2014**, *20*, 103–114. [[CrossRef](#)]
38. Imparato, G.; Urciuolo, F.; Casale, C.; Netti, P.A. The role of micro scaffold properties in controlling the collagen assembly in 3D dermis equivalent using modular tissue engineering. *Biomaterials* **2013**, *34*, 7851–7861. [[CrossRef](#)]
39. Jiang, T.; Deng, M.; Fattah, W.I.A.; Laurencin, C.T. Chitosan-Based Biopharmaceutical Scaffolds in Tissue Engineering and Regenerative Medicine. In *Chitosan-Based Systems for Biopharmaceuticals*; Wiley: Hoboken, NJ, USA, 2012; pp. 393–427.
40. Kopp, J.; Wang, G.Y.; Horch, R.; Pallua, N.; Ge, S.D. Ancient traditional Chinese medicine in burn treatment: A historical review. *Burns* **2003**, *29*, 473–478. [[CrossRef](#)]
41. Kim, S.Y.; Park, B.J.; Lee, Y.; Park, J.N.; Park, K.M.; Hwang, Y.S.; Park, K.D. Human hair keratin-based hydrogels as dynamic matrices for facilitating wound healing. *J. Ind. Eng. Chem.* **2019**, *73*, 142–151. [[CrossRef](#)]
42. Lin, C.-W.; Chen, Y.-K.; Tang, K.-C.; Yang, K.-C.; Cheng, N.-C.; Yu, J. Keratin scaffolds with human adipose stem cells: Physical and biological effects toward wound healing. *J. Tissue Eng. Regen. Med.* **2019**, *13*, 1044–1058. [[CrossRef](#)] [[PubMed](#)]
43. Keskin, Z.; Urkmez, A.S.; Hames, E.E. Novel keratin modified bacterial cellulose nanocomposite production and characterization for skin tissue engineering. *Mater. Sci. Eng. C* **2017**, *75*, 1144–1153. [[CrossRef](#)]
44. Sulaeva, I.; Henniges, U.; Rosenau, T.; Potthast, A. Bacterial cellulose as a material for wound treatment: Properties and modifications. A review. *Biotech. Adv.* **2015**, *333*, 1547–1571. [[CrossRef](#)]
45. Siller-Jackson, A.J.; Van Dyke, M.E.; Timmons, S.F.; Blanchard, C.R. Keratin-Based Powders and Hydrogel for Pharmaceutical Applications. U.S. Patent US6544548B1, 8 April 2003.
46. Blanchard, C.R. Keratin Based Hydrogel for Biomedical Applications. U.S. Patent US5932552, 3 August 1999.
47. Rajwade, J.M.; Paknikar, K.M.; Kumbhar, J.V. Applications of bacterial cellulose and its composites in biomedicine. *Appl. Microbiol. Biotechnol.* **2015**, *99*, 2491–2511. [[CrossRef](#)]
48. Bunnell, B.A.; Flaata, M.; Gagliardi, C.; Patel, B.; Ripoll, C. Adipose-derived stem expansion and differentiation. *Methods* **2008**, *45*, 115–120. [[CrossRef](#)]
49. Schramm, M.; Hestrin, S. Factors affecting production of cellulose at the air/liquid interface of a culture of *Acetobacter xylinum*. *J. Gen. Microbiol.* **1954**, *11*, 123–129. [[CrossRef](#)]
50. Pavlov, K.F.; Romankov, P.G.; Noskov, A.A. *Processes and Apparatus in Chemical Engineering*, 8th ed.; Editura Tehnica: Bucharest, Romania, 1981; p. 529, Table LVII. (In Romanian)
51. Zhang, Q.; Liebeck, B.M.; Yan, K.; Demco, D.E.; Körner, A.; Popescu, C. Alpha-Helix Self-Assembly of Oligopeptides Originated From Beta-Sheet Keratin. *Macromol. Chem. Phys.* **2012**, *213*, 2628–2638. [[CrossRef](#)]
52. Liebeck, B.M.; Hidalgo, N.; Roth, G.; Popescu, C.; Böker, A. Synthesis and Characterization of Methyl Cellulose/Keratin Hydrolysate Composite Membranes. *Polymers* **2017**, *9*, 91. [[CrossRef](#)] [[PubMed](#)]
53. Picheth, G.F.; Pirich, C.L.; Sierakowski, M.R.; Woehl, M.A.; Novak, S.C.; Souza, C.F.; Martin, A.A.; da Silva, R.; de Freitas, R.A. Bacterial cellulose in biomedical applications: A review. *Int. J. Biol. Macromol.* **2017**, *104*, 97–106. [[CrossRef](#)]
54. Aursulesei, V.; Vasincu, D.; Timofte, D.; Vrajitoriu, L.; Gatu, I.; Iacob, D.D.; Ghizdovat, V.; Buzea, C.; Agop, M. New mechanisms of vesicles migration. *Gen. Physiol. Biophys.* **2016**, *35*, 287–298. [[CrossRef](#)]

55. Burlacu, A.; Siriopol, D.; Voroneanu, L.; Nistor, I.; Hogas, S.; Nicolae, A.; Nedelciuc, I.; Tinica, G.; Covic, A. Atherosclerotic Renal Artery Stenosis Prevalence and Correlations in Acute Myocardial Infarction Patients Undergoing Primary Percutaneous Coronary Interventions: Data from Nonrandomized Single-Center Study (REN-ACS)—A Single Center, Prospective, Observational Study. *J. Am. Hear. Assoc.* **2015**, *4*, e002379. [[CrossRef](#)]
56. Hsieh, W.C.; Chen, P.C.; Corciova, F.C.; Tinica, G. Liver dysfunction as an important predicting risk factor in patients un-dergoing cardiac surgery: A systematic review and meta-analysis. *Int. J. Clin. Exp. Med.* **2015**, *8*, 20712–20721.
57. Trofin, F.; Ciobica, A.; Honceriu, C. Modulatory effects of vitamin C on the relation between physical exercising and oxidative stress at young smokers. *Rom. Biotechnol. Lett.* **2017**, *22*, 12439–12447.
58. Al-Tarrah, K.; Moiemmen, N.; Lord, J.M. The influence of sex steroid hormones on the response to trauma and burn injury. *Burn. Trauma* **2017**, *5*, 29. [[CrossRef](#)]